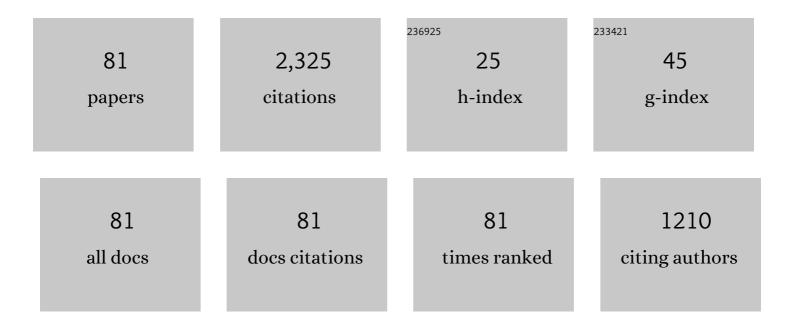
List of Publications by Year in descending order

Source: https://exaly.com/author-pdf/8079792/publications.pdf Version: 2024-02-01



WENRIN XIIF

#	Article	IF	CITATIONS
1	Analyses of electrochemical behavior of plasma electrolytic oxidation film on Zirlo alloy in lithium borate buffer solution at 25–300°C. Surface and Coatings Technology, 2022, 429, 127935.	4.8	5
2	FABRICATION AND WEAR BEHAVIOR OF PEC/N HARDENED LAYER ON PURE IRON. Surface Review and Letters, 2022, 29, .	1.1	0
3	Microstructure and properties of BÂ+ÂCÂ+ÂN ternary hardening layers on Q235 low-carbon steel prepared by plasma electrolysis. Surface and Coatings Technology, 2022, 440, 128505.	4.8	3
4	Microstructural characterizations of γ-TiAl alloy after high-temperature steam oxidations at 900, 1000, 1100 and 1200°C. Materials Characterization, 2022, 189, 111979.	4.4	11
5	Effect of nickel-coated carbon nanotubes on the preparation and wear resistance of microarc oxidation ceramic coating on ZL109 aluminum alloy. Scientific Reports, 2022, 12, .	3.3	0
6	Influence of voltage on growth and microstructure of oxide coatings on Î ³ -TiAl alloy by cathodic plasma electrolysis in glycerin solution. Surface and Coatings Technology, 2022, 444, 128666.	4.8	3
7	High temperature oxidation of Zr 1Nb alloy with plasma electrolytic oxidation coating in 900–1200°C steam environment. Surface and Coatings Technology, 2021, 407, 126768.	4.8	18
8	Effects of Li, B and H elements on corrosion property of oxide films on ZIRLO alloy in 300 °C/14 MPa lithium borate buffer solutions. Corrosion Science, 2021, 181, 109216.	6.6	14
9	Electrochemical Study of TA2 Titanium in a High-Temperature and -Pressure Water Environment. Coatings, 2021, 11, 659.	2.6	2
10	Enhancement of high temperature steam oxidation resistance of Zr–1Nb alloy with ZrO2/Cr bilayer coating. Corrosion Science, 2021, 187, 109494.	6.6	41
11	Steam oxidation behavior of ZrO2/Cr-coated pure zirconium prepared by plasma electrolytic oxidation followed by filtered cathodic vacuum arc deposition. Journal of Alloys and Compounds, 2021, 883, 160798.	5.5	20
12	One-step plasma electrolytic oxidation for TiO ₂ /SnO ₂ film as LIB anode. Surface Engineering, 2021, 37, 918-925.	2.2	2
13	HIGH TEMPERATURE STEAM CORROSION OF MICROARC OXIDATION COATINGS ON 6061 ALUMINUM ALLOY AT 300â ^{~~} C/3 MPa STEAM. Surface Review and Letters, 2021, 28, 2050030.	1.1	1
14	Combination of plasma electrolytic oxidation and pulsed laser deposition for preparation of corrosion-resisting composite film on zirconium alloys. Materials Letters, 2020, 262, 127080.	2.6	21
15	Anticorrosive non-crystalline coating prepared by plasma electrolytic oxidation for ship low carbon steel pipes. Scientific Reports, 2020, 10, 15675.	3.3	13
16	Degradation of 2,4-dichlorophenol by cathodic microarc plasma electrolysis: characteristics and mechanisms. Environmental Technology (United Kingdom), 2020, , 1-13.	2.2	0
17	In-situ electrochemical study of plasma electrolytic oxidation treated Zr3Al based alloy in 300°C/14 MPa lithium borate buffer solution. Thin Solid Films, 2020, 707, 138066.	1.8	15
18	Evolution of carbon diffusion layer to oxidation film during cathodic plasma electrolysis on steel. Heat Treatment and Surface Engineering, 2020, 2, 1-8.	1.0	0

#	Article	IF	CITATIONS
19	Analyses of hydrogen release on zirlo alloy anode during plasma electrolytic oxidation. Materials Chemistry and Physics, 2020, 251, 123054.	4.0	31
20	Influence of microarc oxidation power supply frequency on tribology performance of a self-lubricating coating for Al–Si diesel engine pistons. Materials Research Express, 2019, 6, 1165a7.	1.6	5
21	Influence of temperature on tribological properties of microarc oxidation coating on 7075 aluminium alloy at 25†°C –300†°C. Ceramics International, 2019, 45, 12312-12318.	4.8	34
22	Fabrication and optical emission spectroscopy of enhanced corrosion-resistant CPEO films on Q235 low carbon steel. Surface and Coatings Technology, 2019, 363, 411-418.	4.8	18
23	Rapid construction of TiO2/SiO2 composite film on Ti foil as lithium-ion battery anode by plasma discharge in solution. Applied Physics Letters, 2019, 114, 043903.	3.3	11
24	Tribological properties of microarc oxidation coatings on Zirlo alloy. Surface Engineering, 2019, 35, 692-700.	2.2	16
25	Temperature measurement and OES analysis during CPEO on stainless steel. Surface and Coatings Technology, 2019, 363, 314-321.	4.8	5
26	Combined treatment plasma electrolytic carburizing and borocarburizing on Q235 low-carbon steel. Materials Chemistry and Physics, 2019, 221, 232-238.	4.0	21
27	In-situ high temperature electrochemical investigation of ZrO2/CrN ceramic composite film on zirconium alloy. Surface and Coatings Technology, 2019, 359, 366-373.	4.8	17
28	Surface charge and corrosion behavior of plasma electrolytic oxidation film on Zr3Al based alloy. Surface and Coatings Technology, 2019, 357, 412-417.	4.8	13
29	Degradation of phenol in wastewater by cathodic microarc plasma electrolysis. Environmental Technology (United Kingdom), 2019, 40, 969-978.	2.2	5
30	Effects of experimental parameters on phenol degradation by cathodic microarc plasma electrolysis. Separation and Purification Technology, 2018, 201, 179-185.	7.9	13
31	Direct growth of oxide layer on carbon steel by cathodic plasma electrolysis. Surface and Coatings Technology, 2018, 338, 63-68.	4.8	15
32	Preparation and tribological behaviors of DLC/spinel composite film on 304 stainless steel formed by cathodic plasma electrolytic oxidation. Surface and Coatings Technology, 2018, 338, 38-44.	4.8	9
33	High temperature tribological behavior of microarc oxidation film on Ti-39Nb-6Zr alloy. Surface and Coatings Technology, 2018, 347, 29-37.	4.8	32
34	Zeta potential of microarc oxidation film on zirlo alloy in different aqueous solutions. Corrosion Science, 2018, 143, 129-135.	6.6	25
35	Characterization of plasma electrolytic oxidation film on biomedical high niobium-containing β‑titanium alloy. Surface and Coatings Technology, 2018, 352, 295-301.	4.8	17
36	FABRICATION AND CHARACTERIZATION OF PLASMA ELECTROLYTIC BOROCARBURIZED LAYERS ON Q235 LOW-CARBON STEEL AT DIFFERENT DISCHARGE VOLTAGES. Surface Review and Letters, 2017, 24, 1750088.	1.1	3

#	Article	IF	CITATIONS
37	EFFECT OF DISCHARGE TIME ON PLASMA ELECTROLYTIC BOROCARBONITRIDING OF PURE IRON. Surface Review and Letters, 2017, 24, 1750016.	1.1	4
38	Investigation of anodic plasma electrolytic carbonitriding on medium carbon steel. Surface and Coatings Technology, 2017, 313, 288-293.	4.8	20
39	Optical emission spectroscopy of plasma electrolytic oxidation process on 7075 aluminum alloy. Surface and Coatings Technology, 2017, 324, 18-25.	4.8	35
40	Characterization and first-principles calculations of WO 3 /TiO 2 composite films on titanium prepared by microarc oxidation. Materials Chemistry and Physics, 2017, 201, 311-322.	4.0	17
41	Fabrication and characterization of microarc oxidation films on Ti-39Nb-6Zr alloy at different voltages in KOH electrolyte. Journal of Alloys and Compounds, 2017, 725, 1158-1165.	5.5	18
42	Cathodic plasma electrolysis for preparation of diamond-like carbon particles in glycerol solution. Materials Chemistry and Physics, 2017, 199, 289-294.	4.0	9
43	Enhanced wear and corrosion resistance of plasma electrolytic carburized layer on T8 carbon steel. Materials Chemistry and Physics, 2016, 171, 50-56.	4.0	15
44	Influence of discharge time on properties of plasma electrolytic borocarburized layers on Q235 low-carbon steel. Materials Chemistry and Physics, 2015, 168, 10-17.	4.0	10
45	Preparation and characterization of carburized layer on pure aluminum by plasma electrolysis. Surface and Coatings Technology, 2015, 269, 119-124.	4.8	13
46	Analyses of reinforcement phases during plasma electrolytic oxidation on magnesium matrix composites. Surface and Coatings Technology, 2015, 269, 212-219.	4.8	23
47	Anti-corrosion layer prepared by plasma electrolytic carbonitriding on pure aluminum. Applied Surface Science, 2015, 347, 673-678.	6.1	28
48	High-temperature oxidation of Q235 low-carbon steel treated by plasma electrolytic borocarburizing. Surface and Coatings Technology, 2015, 269, 302-307.	4.8	18
49	INFLUENCE OF MICROSTRUCTURE OF FRICTION STIR WELDED JOINTS ON GROWTH AND PROPERTIES OF MICROARC OXIDATION COATINGS ON AZ31B MAGNESIUM ALLOY. Surface Review and Letters, 2015, 22, 1550029.	1.1	2
50	The effect of microarc oxidation and excimer laser processing on the microstructure and corrosion resistance of Zr–1Nb alloy. Journal of Nuclear Materials, 2015, 467, 186-193.	2.7	25
51	Corrosion behavior of friction stir welded AZ31B magnesium alloy with plasma electrolytic oxidation coating formed in silicate electrolyte. Materials Chemistry and Physics, 2014, 144, 462-469.	4.0	37
52	Characterization of carburized layer on T8 steel fabricated by cathodic plasma electrolysis. Surface and Coatings Technology, 2014, 245, 9-15.	4.8	45
53	Spectroscopic investigation of plasma electrolytic borocarburizing on q235 low-carbon steel. Applied Surface Science, 2014, 321, 348-352.	6.1	20
54	Analyses of quenching process during turn-off of plasma electrolytic carburizing on carbon steel. Applied Surface Science, 2014, 316, 102-107.	6.1	25

#	Article	IF	CITATIONS
55	Discharge behaviors during plasma electrolytic oxidation on aluminum alloy. Materials Chemistry and Physics, 2014, 148, 284-292.	4.0	63
56	Characterization of surface hardened layers on Q235 low-carbon steel treated by plasma electrolytic borocarburizing. Journal of Alloys and Compounds, 2013, 578, 162-169.	5.5	60
57	Preparation and characterization of diamond-like carbon/oxides composite film on carbon steel by cathodic plasma electrolysis. Applied Physics Letters, 2013, 103, .	3.3	22
58	High temperature tribological behaviors of plasma electrolytic borocarburized Q235 low-carbon steel. Surface and Coatings Technology, 2013, 232, 142-149.	4.8	47
59	Effect of voltage on properties of microarc oxidation films prepared in phosphate electrolyte on Zr–1Nb alloy. Surface and Coatings Technology, 2013, 222, 62-67.	4.8	62
60	Characterization of wear-resistant coatings on 304 stainless steel fabricated by cathodic plasma electrolytic oxidation. Surface and Coatings Technology, 2013, 236, 22-28.	4.8	30
61	Microbial influenced corrosion behavior of micro-arc oxidation coating on AA2024. Surface and Coatings Technology, 2013, 216, 100-105.	4.8	26
62	DUPLEX Al2O3/DLC COATING ON 15SiCp/2024 ALUMINUM MATRIX COMPOSITE USING COMBINED MICROARC OXIDATION AND FILTERED CATHODIC VACUUM ARC DEPOSITION. Surface Review and Letters, 2012, 19, 1250036.	1.1	3
63	Characterization of ceramic coatings fabricated on zirconium alloy by plasma electrolytic oxidation in silicate electrolyte. Materials Chemistry and Physics, 2010, 120, 656-660.	4.0	91
64	PREPARATION OF MICROARC OXIDATION COATINGS ON 6061 ALUMINUM ALLOYS AND THEIR THERMAL SHOCK RESISTANCE. Surface Review and Letters, 2009, 16, 393-399.	1.1	1
65	New Four-Band Electrode Fabrication To Measure in Situ Electrical Property of Conducting Polymers. Analytical Chemistry, 2009, 81, 2364-2372.	6.5	11
66	Al2O3 coating fabricated on titanium by cathodic microarc electrodeposition. Journal of Alloys and Compounds, 2009, 476, 356-359.	5.5	19
67	Anti-corrosion microarc oxidation coatings on SiCP/AZ31 magnesium matrix composite. Journal of Alloys and Compounds, 2009, 482, 208-212.	5.5	54
68	Corrosion behaviors and galvanic studies of microarc oxidation films on Al–Zn–Mg–Cu alloy. Surface and Coatings Technology, 2007, 201, 8695-8701.	4.8	64
69	Preparation of anti-corrosion films by microarc oxidation on an Al–Si alloy. Applied Surface Science, 2007, 253, 6118-6124.	6.1	86
70	Three-dimensional grain size distribution: Comparison of an analytical form under a topology-related rate equation with computer simulations and experimental data. Materials Science & Engineering A: Structural Materials: Properties, Microstructure and Processing, 2007, 454-455, 547-551.	5.6	14
71	On the quasi-stationary grain size distribution from two Gamma size distributions in three-dimensional grain growth. Materials Letters, 2007, 61, 4262-4266.	2.6	5
72	Anti-corrosion film on 2024/SiC aluminum matrix composite fabricated by microarc oxidation in silicate electrolyte. Journal of Alloys and Compounds, 2006, 425, 302-306.	5.5	65

#	Article	IF	CITATIONS
73	Tribological Behavior of Microarc Oxidation Coatings on Aluminum Alloy. ISIJ International, 2006, 46, 287-291.	1.4	22
74	Features of film growth during plasma anodizing of Al 2024/SiC metal matrix composite. Applied Surface Science, 2006, 252, 6195-6200.	6.1	29
75	Analyses of Microarc Oxidation Coatings Formed on Si-containing Cast Aluminum Alloy in Silicate Solution ISIJ International, 2002, 42, 1273-1277.	1.4	19
76	Characterization of Oxide Coatings Deposited on Pure Titanium by Alternating-current Microarc Discharge in Electrolyte ISIJ International, 2002, 42, 651-655.	1.4	5
77	Evaluation of the mechanical properties of microarc oxidation coatings and 2024 aluminium alloy substrate. Journal of Physics Condensed Matter, 2002, 14, 10947-10952.	1.8	41
78	Structure and properties characterization of ceramic coatings produced on Ti–6Al–4V alloy by microarc oxidation in aluminate solution. Materials Letters, 2002, 52, 435-441.	2.6	164
79	Title is missing!. Journal of Materials Science, 2001, 36, 2615-2619.	3.7	49
80	Growth regularity of ceramic coatings formed by microarc oxidation on Al–Cu–Mg alloy. Thin Solid Films, 2000, 372, 114-117.	1.8	240
81	Analysis of Phase Distribution for Ceramic Coatings Formed by Microarc Oxidation on Aluminum Alloy. Journal of the American Ceramic Society, 1998, 81, 1365-1368.	3.8	210